

# Functionally gradient ceramic/metallic coatings for gas turbine components by high-energy beams for high-temperature applications

D. WOLFE, J. SINGH

*Applied Research Laboratory, Engineering Science and Mechanics,  
The Pennsylvania State University, University Park, PA 16904, USA  
E-mail: dew125@psu.edu, jxs46@psu.edu*

Failure of turbine blades generally results from high-temperature oxidation, corrosion, erosion, or combinations of these procedures at the tip, and the leading and trailing edges of a turbine blade. To overcome these limitations, functionally gradient ceramic/metallic coatings have been produced by high-energy beams for high-temperature applications in the aerospace and turbine industries to increase the life of turbine components. Thermal spray processes have long been used to apply high-temperature thermal barrier coatings to improve the life of turbine components. However, these processes have not met the increased demand by the aerospace and turbine industries to obtain higher engine temperatures and increased life enhancement as a result of the inhomogeneous microstructure, unmelted particles, voids, and poor bonding with the substrate. High-energy beams, i.e. electron beam-physical vapour deposition (EB-PVD), laser glazing, laser surface alloying, and laser surface cladding, have been explored to enhance the life of turbine components and overcome the limitations of the thermal spray processes. EB-PVD has overcome some of the disadvantages of the thermal spray processes and has increased the life of turbine components by a factor of two as a result of the columnar microstructure in the thermal barrier coating (TBC). Laser glazing has been used to produce metastable phases, amorphous material, and a fine-grained microstructure, resulting in improved surface properties such as fatigue, wear, and corrosion resistance at elevated temperatures without changing the composition of the surface material. Laser surface alloying and laser surface cladding have shown promising results in improving the chemical, physical, and mechanical properties of the substrate's surface. Metal-matrix composite coatings have also been produced by a laser technique which resulted in increased wear- and oxidation-resistant properties. The advantages and disadvantages of thermal spray processes, EB-PVD, laser glazing, laser surface alloying, and laser surface cladding will be discussed. Microstructural evolution of thermal barrier coatings, recent advancements in functionally gradient coatings, laser grooving, and multilayered textured coatings will also be discussed. © 1998 Kluwer Academic Publishers

## 1. Introduction

Aerospace and power-generating gas turbine industries are continuously putting effort into increasing the thermal efficiency of the engine, as well as the life of turbine components under severe environmental conditions such as wear, corrosion, and oxidation at elevated temperatures. The performance of turbine components can be increased by improving the cooling path within the turbine components (such as blades or airfoils), developing new heat-resistant materials, applying coatings, or a mixed combination. In fact, coatings are playing a significant role in today's military and gas turbine engines to extend the life or enhance the performance of components. About 75%

of all the components in the jet engine are coated. Thus, the selection of coating materials and processes is important for specific applications and performance. Coatings can also be sacrificial, as in the case of certain abrasion-resistant coatings for seal systems in a jet engine. In all cases, however, the coating is applied to enhance the life and performance of the component without significant detrimental effect on the basic mechanical and physical properties of the underlying material.

It is very difficult to generalize the nature of damage occurring in various turbine components such as combustors, vanes, and blades. Among turbine components, turbine blades require a constant maintenance

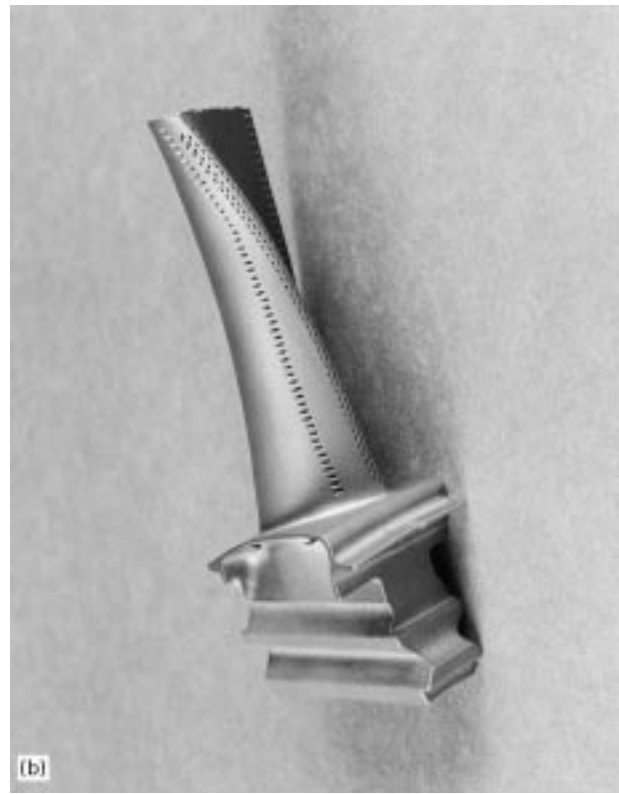
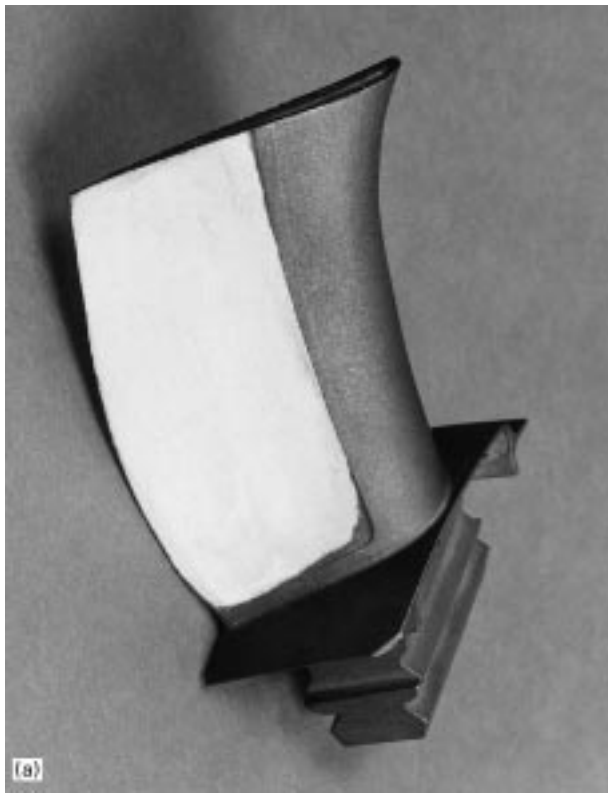


Figure 1 Photographs of a turbine blade.

including repair, refurbishment, and even replacement. Before proceeding further, it is important to review the most probable damage areas: the tip, and the leading and trailing edges of the turbine blade (Fig. 1). The tip damage is predominantly the result of high-temperature wear or rubbing against the stator liner coatings, i.e. abradable seal coatings. When turbine blades are rotated at high speeds and subjected to high-temperature exposure, the dimensions of the turbine blades changes. Owing to thermal expansion in the turbine blades, the tip rubs against the stator liner. Although, the stator liner is coated with soft abradable coatings, the turbine tip still wears out due to rubbing at high temperatures. In the rubbing event, the temperature of the turbine tip is much higher than the engine operating temperature. Tip performance is generally enhanced by applying wear-resistant coatings. Plasma spraying or laser cladding are commonly used to apply wear-resistant coatings. Details of each process will be discussed below along with their advantages and disadvantages.

Damage in the leading and trailing edges of turbine blades occurs due to either high-temperature oxidation, corrosion, erosion, or combinations of these procedures. The performance of materials is restricted by its surface properties and thermal stability that can be enhanced by applying metallic and ceramic coatings. The most common metallic coatings used in the hot section of a turbine engine are M 10–25% Cr 6–11% Al–1% Y or Hf (M = Ni, Co, Fe) alloys and thermal barrier coatings [1,2]. MCrAlY alloys are used as they have good oxidation and corrosion-resistant properties at elevated temperatures. Thermal barrier coatings (TBC) are used for thermal protection in

order to operate the engine at high temperatures. These coatings are generally applied by either the plasma spray or electron beam-physical vapour deposition (EB-PVD) processes.

The turbine industries must face two challenges: the selection of the coating process and the selection of coating materials. The above-mentioned coating materials and processes have been used in the turbine industry for over two decades. Now, the new thrust of the turbine industry is to operate the engine (hot section) at much higher temperatures, i.e. from 1420–1600 K with an ultimate goal of up to 1750 K. The selection of coating materials and processes are the key to the success of this mission. In this paper, different coating processes will be reviewed, followed by coating materials for specific applications and their advancements.

## 2. Thermal spray processes

In the thermal spray processes, pre-alloyed powder or wire is melted in the hot flame (plasma) and transferred along with the high-pressure carrier gas (Fig. 2). The plasma is generated by using chemical combustion gases or electrical (arc) energy to produce plasma jets with temperature distributions of 3000–15000 K. At these temperatures, the plasma gas (argon, helium, hydrogen, nitrogen) dissociates and ionizes into an equilibrium mixture of ions and electrons. This plasma energy melts any material to its melting point. Owing to the continuous stream of pressurized gas and plasma formation, molten material is finely divided into millions of droplets that travel at velocities exceeding  $6000 \text{ ft s}^{-1}$  ( $1 \text{ ft s}^{-1} = 3.0480 \times 10^{-1} \text{ m s}^{-1}$ ).

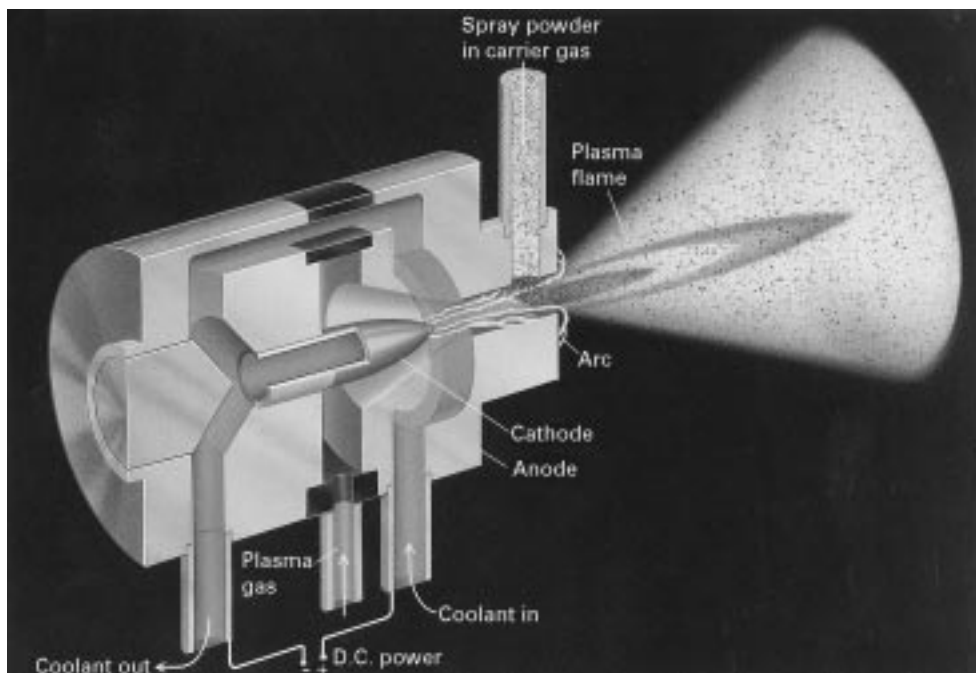


Figure 2 Schematic diagram of the plasma spray process [3].

High-speed droplets are projected towards the substrate. Molten particles impact the substrate and deform into lamellar splats. Each droplet is basically deformed during solidification; droplets rapidly build up particle by particle as they impact the target forming continuous solid layers. Each individual splat is typically thin (1–20  $\mu\text{m}$ ), and the droplets cool at very high rates ( $\sim 10^6 \text{ K s}^{-1}$  for metals) to form a coating. Because millions of particles are exposed simultaneously in the flame or plasma, many particles do not experience the same heating. Some particles may not be melted at all, resulting in porosity, or trapped unmelted particles in the coating. Consolidation of particles occurs through liquid flow, solid redistribution, solid formation, recrystallization, and diffusion. In many cases, the continuous bombardment of newly deposited surfaces by subsequent impacting particles will result in locally densifying deposits through mechanical working or the peening effect [4]. All of these consolidation steps are driven by thermomechanical energy intrinsic to various thermal spray processes. The property of the coating depends on various factors, including the type of thermal spray processes

used, the operating conditions selected, and the material being sprayed. Thermal spray processes can be subclassified based on the heat energy and plasma formation, i.e. thermal spray, plasma spray, low-pressure vacuum plasma spray, detonation gun (D-gun), and high-velocity oxyfuel (HVOF) processes [5]. The plasma energy depends upon the type of combustion gas used in the processes. For example, in the HVOF process, an internal combustion jet composed of acetylene, propylene, hydrogen, or propane, produces hypersonic gas velocities of about  $6000 \text{ ft s}^{-1}$  or five times the speed of sound. Typical properties of 88% WC–12% Co coating produced by different processes are given in Table I [6].

Significant advantages of these processes are the high deposition rates ( $100\text{--}1000 \mu\text{m min}^{-1}$ ) and the various metallic and oxide coatings that can be applied. Disadvantages of the spray processes are the inability to obtain homogeneous and dense microstructures. In addition, the coating surface is relatively rough. Coatings contain defects such as microporosity, non-bonded interfaces, and grain-boundary precipitation. These defects in the microstructure may

TABLE I Typical properties of WC–Co coating produced by different processes

|   | HVOF D-Gun | Standard | High-Velocity Plasma | Plasma |
|---|------------|----------|----------------------|--------|
| Flame temperature ( $^{\circ}\text{C}$ )    | 2760       | 2760     | 11100                | 11100  |
| ( $^{\circ}\text{F}$ )                      | 5000       | 5000     | 20000                | 20000  |
| Gas velocity                                | Mach 4     | Mach 3   | Subsonic             | Mach 1 |
| Porosity (%)                                | 0          | < 1      | < 2                  | < 1    |
| Oxide content                               | < 1        | < 1      | < 3                  | < 1    |
| Typical bond strength (p.s.i.) <sup>a</sup> | 10000      | 10000    | 8000                 | 10000  |
| Thickness limitation (in) <sup>b</sup>      | 0.060      | 0.030    | 0.025                | 0.015  |

<sup>a</sup>  $10^3 \text{ p.s.i.} = 6.89 \text{ N mm}^{-2}$ .

<sup>b</sup>  $1 \text{ m} = 2.54 \text{ cm}$ .

result in lower mechanical properties such as ductility, resistance to wear, corrosion, oxidation, and impact [4].

### 3. Electron beam-physical vapour deposition

Some of the shortcomings in the thermal spray processes were overcome by electron beam-physical vapour deposition (EB-PVD) process [6, 7]. In the EB-PVD process, focused high-energy electron beams generated from electron guns are directed to melt and evaporate ingots as well as to preheat the substrate inside the vacuum chamber (as shown in Fig. 3). The vapour cloud condenses on the substrate and forms the coating. To obtain more uniform coatings, the sample is often rotated in the vapour cloud during the coating process. In addition, non-uniform deposition is reduced by scanning the electron beam over the surface of the melt pool. The depth of the melt and degree of vaporization can be controlled by restricting the kinetic energy of the electron beam. Such a restriction allows deposition rates to range from  $0.1 \text{ nm s}^{-1}$  to as high as  $150 \text{ } \mu\text{m min}^{-1}$  (for metals). Because the evaporated material does not come into contact with the crucible, coatings of high purity are produced with this technology.

#### 3.1 Advantages of EB-PVD

The EB-PVD process offers many desirable characteristics such as relatively high deposition rates (up to  $100\text{--}150 \text{ } \mu\text{m min}^{-1}$  with an evaporation rate  $\sim 10\text{--}15 \text{ kg h}^{-1}$ ), dense coatings, strong metallurgical bonding (due to higher deposition temperatures), precise composition control, columnar and polycrystalline microstructure, low contamination, and high thermal efficiency. It is a robust process, i.e. the microstructure of the coating is reproducible. Even elements with low vapour pressures such as molybdenum, tungsten, and

carbon are readily deposited by this process. Multi-layered metallic and ceramic coatings (oxides, carbides, nitrides) can be deposited on large components at relatively low temperatures by changing the EB-PVD processing conditions such as ingot composition, part manipulation, and electron beam energy. In addition, the coating surface is relatively smooth [8, 9].

### 4. Ion-beam-assisted EB-PVD

In this process, reactive gas such as nitrogen, oxygen, or argon is passed through an ion beam source where it becomes ionized. These ionized species are mixed or reacted with the evaporated material at the substrate surface, resulting in a good quality coating. This procedure is also called the ion beam-assisted deposition (IBAD) process [10–12]. The attachment of an ion beam source to the EB-PVD equipment also offers additional benefits such as dense coatings with improved adhesion. In addition, textured coatings can be obtained. The state of the internal stresses developed in the coating can be changed from tensile to compressive stress by the forcible injection of high-energy ions (i.e. similar to ion implantation). Thus, the ability to control the stress level in multilayered coatings is an additional feature of ion beam-assisted processing. In addition, a high-energy ion beam (as a source of energy) can be used to clean the surface of the specimen inside the vacuum chamber prior to deposition. This cleaning enhances the metallurgical bonding strength between the coating and the substrate.

### 5. Laser glazing, alloying and cladding

The capability of lasers to be used as tools for materials processing has already been demonstrated [13, 14]. Processes such as laser glazing and laser cladding have successfully demonstrated the synthesis of novel materials in near net shapes.

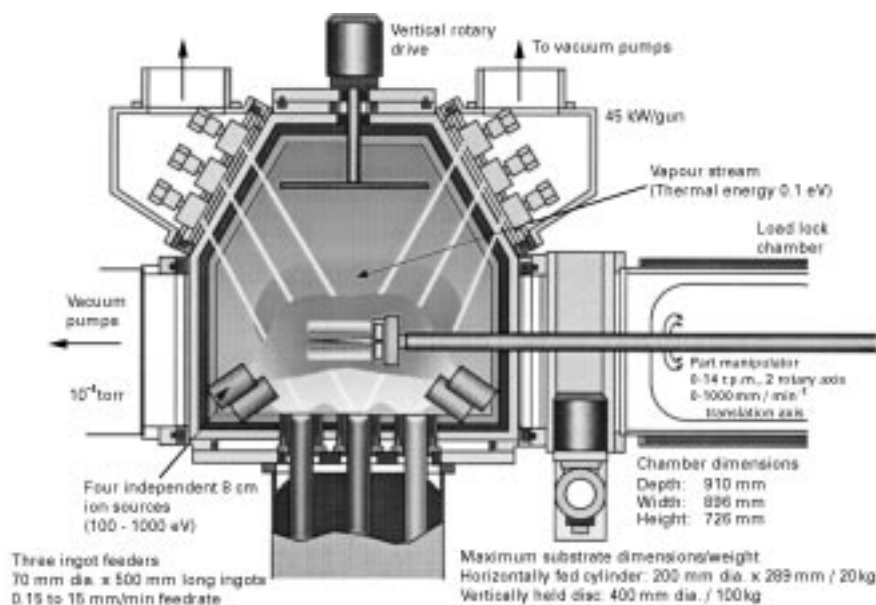


Figure 3 A schematic drawing of an ion beam-assisted 270 kw electron beam PVD process.

In the laser melting and coating processes, the laser energy is absorbed by the surface of the solid and melts the surface. The melt front propagates into the bulk to a depth determined by laser energy input and the materials' properties. The melt velocity is controlled by the rate of energy deposition, the absorbed depth in the solid and liquid phases, and the thermal properties of the solid. After the surface has been melted, the molten layer resolidifies as heat flows into the underlying substrate. When resolidification occurs at the liquid–solid interface, the interface moves to the sample surface with a resolidification velocity  $v$ . Because of the high-temperature gradients,  $v$  can be very large. Temperature gradients ( $\partial T/\partial Z$  where  $Z$  is distance) of up to  $10^{19}$  K  $\text{cm}^{-1}$  and corresponding quenching rates of up to  $10^{11}$  K  $\text{s}^{-1}$  can be readily achieved. An increase in  $\partial T/\partial Z$  results from an increase in  $v$  up to  $20$  m  $\text{s}^{-1}$ . Generally, the microstructure of the laser-irradiated area is characterized as either amorphous, microcrystalline, or epitaxial growth, and its structure depends upon the chemistry of the material, the melting, solidification rates, and laser-processing conditions.

### 5.1. Laser process variables

Applications and efficiency of laser surface treatments depend on *independent* process variables. The key independent process variables are the wavelength of the laser beam, laser power, pulse or CW laser, size and shape of the laser beam, traverse speed of the substrate

with respect to the laser beam, reflectivity/absorbivity of the laser beam, and powder feed rate (for laser surface alloying and cladding). *Dependent* process variables, which are controlled by the above process conditions, are interaction time and cooling rate. Additional cooling can be achieved by applying a copper chilled block to the substrate. Thus, a scheme is needed to develop optimized properties of the materials. Through the manipulation of laser-processing conditions (Fig. 4), a single laser can perform several functions. Such versatility explains why the laser is a popular candidate for a flexible manufacturing system.

### 5.2. Laser glazing

The laser glazing process is used to modify the surface properties of materials. A thin surface layer is rapidly melted and solidified to produce a fine-grained microstructure different from that of the bulk material. High cooling rates of the molten surface layer can promote the formation of an amorphous material, metastable phases, and a fine-grained microstructure resulting in improved surface properties such as wear, corrosion, and fatigue resistance. The principal advantage of laser glazing is that it alters the microstructure without changing the composition, as compared to laser surface alloying and cladding, which are intended to alter the composition of the surface.

Laser glazing can be done with either a pulsed or a continuous wave (CW) laser. A pulsed laser is often

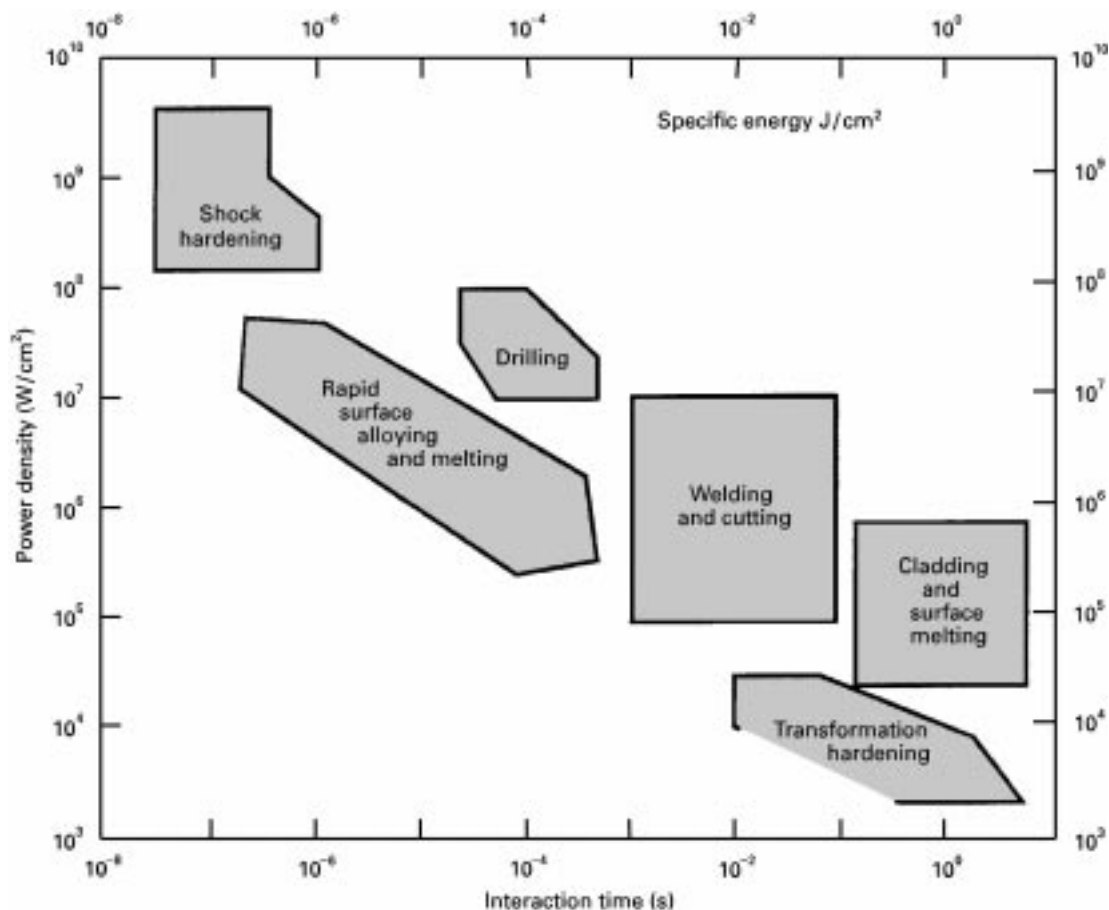


Figure 4 Different regions of laser applications as a function of laser power density and interaction time.

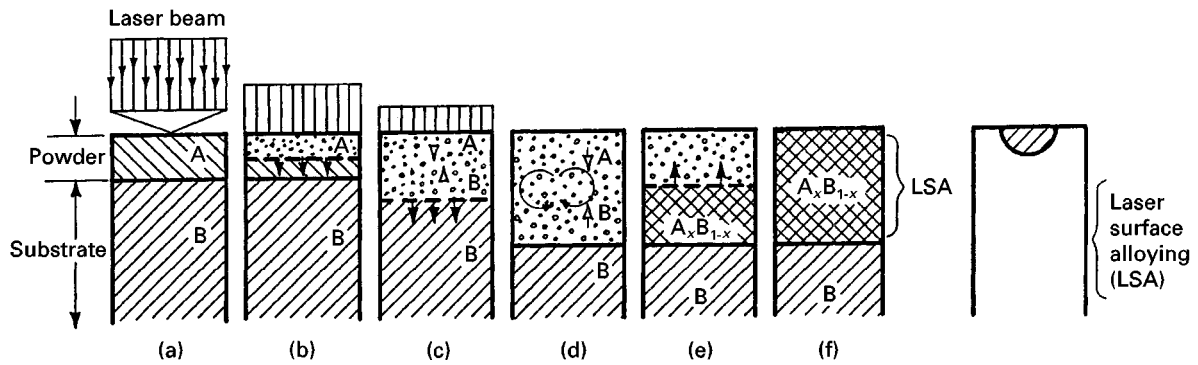


Figure 5 A schematic diagram showing the different steps involved during the laser surface alloying process.

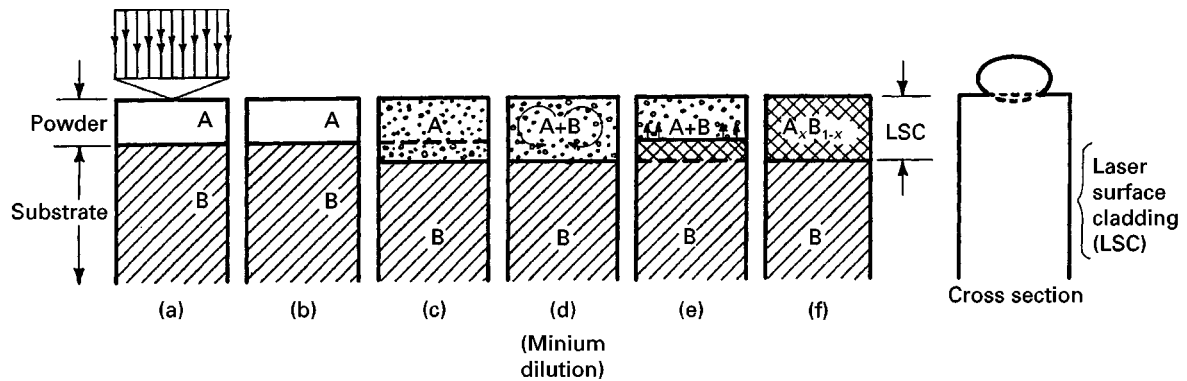


Figure 6 A schematic diagram showing the different steps involved during the laser surface cladding process.

used to achieve very rapid heating (melting) and cooling (solidification) of the near surface of materials with quenching rates of  $10^6$ – $10^{14}$  K s<sup>-1</sup> for metals [15]. The plasma spray process is often used to apply a variety of coatings on parts and also to fabricate near-net shape parts with an anticipation that the properties of the plasma-sprayed component will be equivalent to the wrought alloy. However, the plasma spray coatings contain defects such as porosity, poorly bonded interfaces, and unmelted powder particles that reduce the mechanical properties of the materials. The microstructure, corrosion resistance, and mechanical properties of plasma-coated materials can be improved by the laser glazing process. For example, physical and mechanical properties of the vacuum plasma-sprayed Narloy-Z and thermal barrier coatings (TBC) were improved by the laser glazing process [15].

### 5.3. Laser surface alloying (LSA)

Laser surface alloying is shown in Fig. 5. Consider a pre-placed powder or thin film on the substrate (Fig. 5a), which is then exposed to a laser beam. Depending upon the top surface characteristics of the pre-coated film, a certain amount of energy would be absorbed and instantaneously transferred to the film and substrate. The top surface region rapidly reaches its melting point and transfers the majority of its heat energy to the substrate. A liquid/substrate interface is established and moves towards the substrate, which is the major sink for heat energy (Fig. 5b,c). Within a fraction of a second (<1 ps), the coated film com-

pletely melts and forms a molten region inside the substrate (Fig. 5d). The depth of the melt region depends upon the laser power and interaction time. At this stage, interdiffusion, or mixing, of the precoated thin film with the substrate melt region occurs through a convective fluid flow mechanism. For a fraction of a second, the liquid/solid interface is stationary (Fig. 5d), and then resolidification occurs rapidly. During rapid solidification, the solid/liquid interface moves upwards, as shown in Fig. 5e. Interdiffusion in the liquid melt region continues until it is completely solidified. As the rate of solidification is very high, interdiffusion in the solid state is negligible. The alloy of A and B is thus produced in the substrate (Fig. 5f). The cross-section of the substrate would clearly reveal the formation of the new alloy (having a composition  $A_xB_{1-x}$  within the substrate).

The modified surface thus produced can have superior chemical, physical, or mechanical properties. The depth of the alloy zone can be controlled by the power and the dwell time of the laser beam. Depending upon the type of alloy required at the surface, a less expensive base material can be locally modified to improve resistance to corrosion, erosion, wear, and oxidation.

### 5.4. Laser surface cladding (LSC)

Laser surface cladding is a process similar to laser surface alloying except that dilution by the substrate material is kept to a minimum (Fig. 6a–f). In addition, a clad layer is formed on the substrate surface. Similar

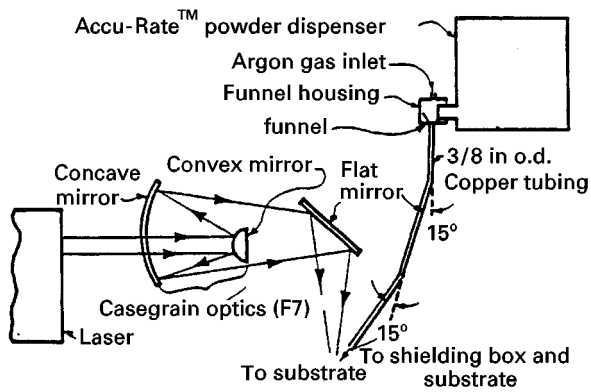


Figure 7 A schematic diagram showing the side delivery of pre-alloyed powder into the melt pool region of the substrate.

to LSA, this process also provides tailored surface properties. By this process, the corrosion, wear, and oxidation resistance can be improved.

Laser cladding has many advantages over alternative methods, such as plasma spraying and arc welding. These advantages include a reduction in dilution, a reduction in waste due to thermal distortion (very little energy is absorbed by the substrate in comparison with plasma spraying and arc welding), a reduction in porosity, and a reduction in post-cladding machining costs. Because the material can be accurately placed, a rapidly solidified microstructure is possible and a relatively smooth surface is produced. Laser cladding offers the potential for generating new materials with metastable phases (e.g. extended solid solution due to the inherent rapid solidification associated with the process).

In laser cladding and alloying processes, alloy wire or powder is transported by an inert gas stream and injected through a nozzle directly into the centre of the laser beam/molten pool and on to the moving substrate. The powder can be delivered into the melt pool region by two methods:

- (i) injecting the powder at an angle into the melt pool region (Fig. 7); or
- (ii) injecting into the melt pool region co-axially along with the laser beam.

A uniform clad layer is produced by both methods.

## 6. Applications

Nickel-based alloys are commonly used as high-temperature environmentally resistant materials in the turbine industries. Three challenges for the nickel-based alloys exist: high-temperature thermal stability, oxidation resistance, and high-temperature mechanical properties. In addition, better high-temperature, wear-resistant properties are needed at the blade tips. The selection of coating processes and materials is very important for enhancing the life of turbine blades and is very critical for each application. For example, turbine blades often rub against the engine liner casing due to thermal expansion and rotation. The tip of the turbine blade has to have high thermal stability as the oxidation process is complex. Various processing techniques have been used in tip alloy development,

such as ion-beam mixing, laser surface alloying, and laser surface cladding, but each process has its own merits. The laser cladding process gave the most promising results in improving the oxidation resistance of nickel-based superalloys. Coatings applied by other processes (such as the plasma spray process) have been reported to have limited life due to poor metallurgical bonding, different microstructures, and a sharp interface between the coating and the substrate. Similarly, coating materials and process selection criteria are different for the leading and trailing edge of turbine blades. Thermal barrier coatings are applied on the skin of turbine blades for thermal protection. Advancements in the coating processes and applications are discussed below.

### 6.1. Environmentally resistant turbine blade-tip coatings by laser cladding

Recently, considerable attention has been given to extending the solid solubility limits of rare-earth additions (e.g. yttrium, rhenium hafnium and cerium) in nickel-based superalloys to improve their oxidation-resistant properties at elevated temperatures. In addition, there has been a continuous effort to disperse rare-earth elements into the nickel-matrix for higher thermal stability. Under equilibrium conditions, the maximum solid solubility of rare-earth metals (hafnium, rhenium, yttrium, cerium) is  $< 0.2 \text{ wt}\%$  at room temperature. Recently, alloys produced by laser surface cladding of Ni-Cr-Al-Hf-Re resulted in a uniform distribution of alloying elements in the clad matrix with an extended solid solubility of alloying additions, a greatly refined microstructure, and the formation of metastable rhenium- and hafnium-rich phases [16–18]. In the laser-clad Ni-Cr-Al-Hf-Re alloys, the main phases are gamma (nickel-based matrix), gamma prime ( $\text{Ni}_3\text{Al}$  structure), and rhenium- and hafnium-rich precipitates (Fig. 8). In addition, a uniform distribution of undissolved hafnium particles into the laser-clad matrix was obtained (Fig. 9) [19–21].

The volume fraction and size of the second phases (e.g. gamma prime) present in the laser-clad matrix depend upon the laser-processing conditions (Fig. 10). The size of the gamma prime precipitates depends upon the hafnium concentration present within, and it increased as the hafnium content increased (Fig. 11). The morphology of gamma prime precipitates also depends upon the rate of solidification and its microchemistry (Fig. 12). Owing to rapid solidification that occurred during laser cladding, the solid solubility of hafnium was increased to  $\sim 30 \text{ wt}\%$  in the gamma prime precipitates (Fig. 13). Thermal stability of the clad alloy depends upon the volume fractions of metastable phases, undissolved hafnium powder particles present, and solid solubility of the alloying additions in the gamma prime precipitates. The thermal stability of a laser-clad Ni-Cr-Al-Hf alloy was found to be  $\sim 1550 \text{ K}$ , which was higher than the nickel-based Rene 95.

It is evident from these results that the laser cladding is a non-equilibrium process by which the

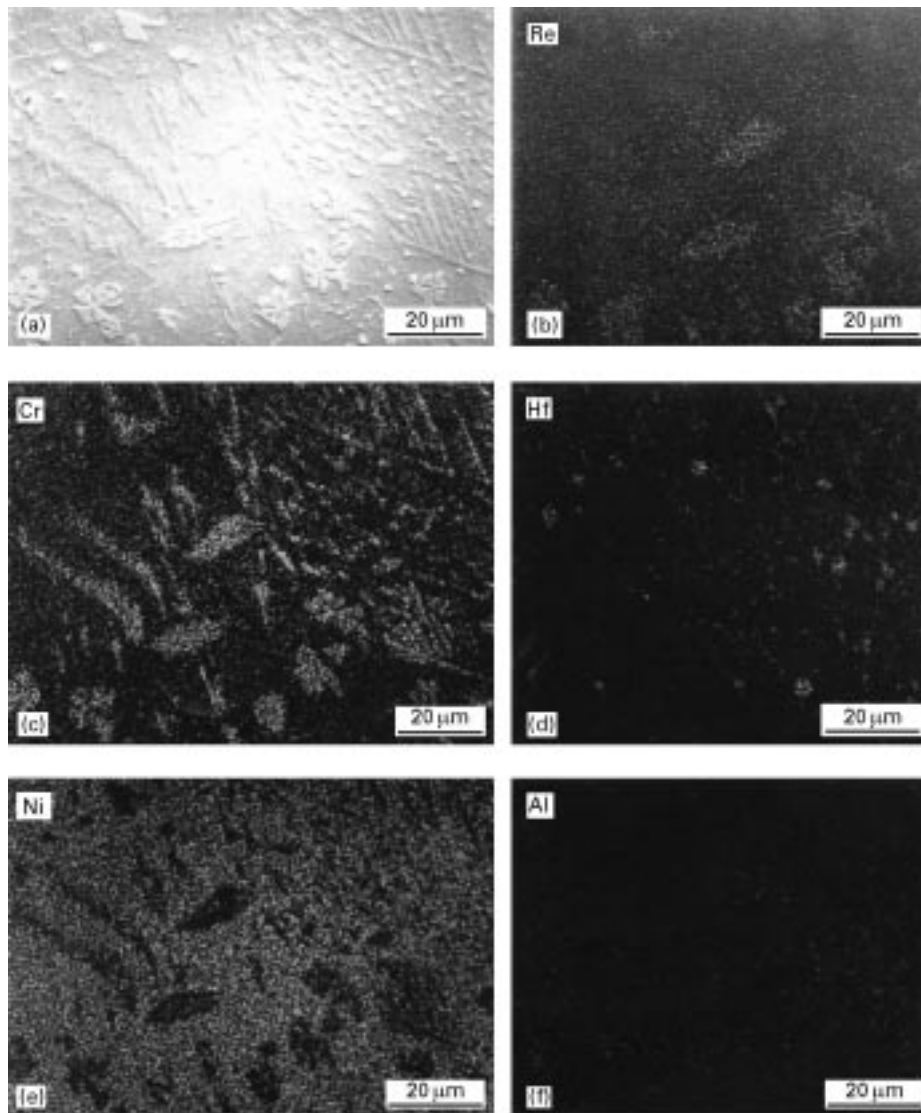


Figure 8 SEM showing the uniform distribution of alloying elements in the laser cladding of a Ni-Cr-Al-Hf-Re alloy.

thermal stability of an alloy can be extended by the addition of high-temperature alloying elements. In addition, the laser-cladding process produces an indistinctive interface between the coating and the substrate.

## 6.2. Advancement in the laser cladding coatings

To meet the new challenges and operate the turbine components at much higher temperatures, metal-matrix composite coatings are being considered to obtain better wear- and oxidation-resistant properties. These coatings should have a uniform dispersion of wear-resistant ceramic powder particles (such as  $\text{Al}_2\text{O}_3$ ,  $\text{HfC}$ ,  $\text{SiC}$ , etc.) into the oxidation-resistant nickel-based matrix. The composite coating was developed by injecting pre-alloyed powder of Ni-Cr-Al-Hf coaxially along with the laser beam into the melt pool region. Simultaneously, the wear-resistant ceramic particles (e.g.  $\text{Al}_2\text{O}_3$ ) were injected at an angle into the melt region, and away from the laser-melt region (as shown in Fig. 14). The ceramic particles were not exposed, nor interacted with the laser

beam. Owing to rapid solidification, the ceramic particles were entrapped within the matrix as shown in Fig. 15. The volume fraction and distribution of the ceramic particles entrapped in the matrix were also dependent upon the laser-processing conditions as previously discussed. Fig. 15 shows a uniform distribution of ceramic  $\text{Al}_2\text{O}_3$  particles in the nickel matrix (Ni-Cr-Al-Hf alloy). Additional rapid quenching rates were achieved using a copper chill block that further refined the microstructure of the clad alloy with an extended solid solubility and a minimum heat-affected zone. Thus, new engineering materials can be tailored by the laser-cladding process and can meet the challenges of turbine industries.

## 6.3. Thermal barrier coatings (TBCs)

Ceramic coatings are continuously gaining importance for high-temperature structural applications because of their excellent mechanical, thermal, and chemical properties. Based on engineering applications, ceramics can be divided into three groups: oxides ( $\text{Al}_2\text{O}_3$ ,  $\text{ZrO}_2$ ,  $\text{SiO}_2$ , etc.), nitrides ( $\text{TiN}$ ,  $\text{SiN}$ ,  $\text{AlN}$ ,  $\text{CrN}$ , etc.), and carbides ( $\text{TiC}$ ,  $\text{SiC}$ ,  $\text{AlC}$ ,  $\text{ZrC}$ ,  $\text{HfC}$ , etc.).



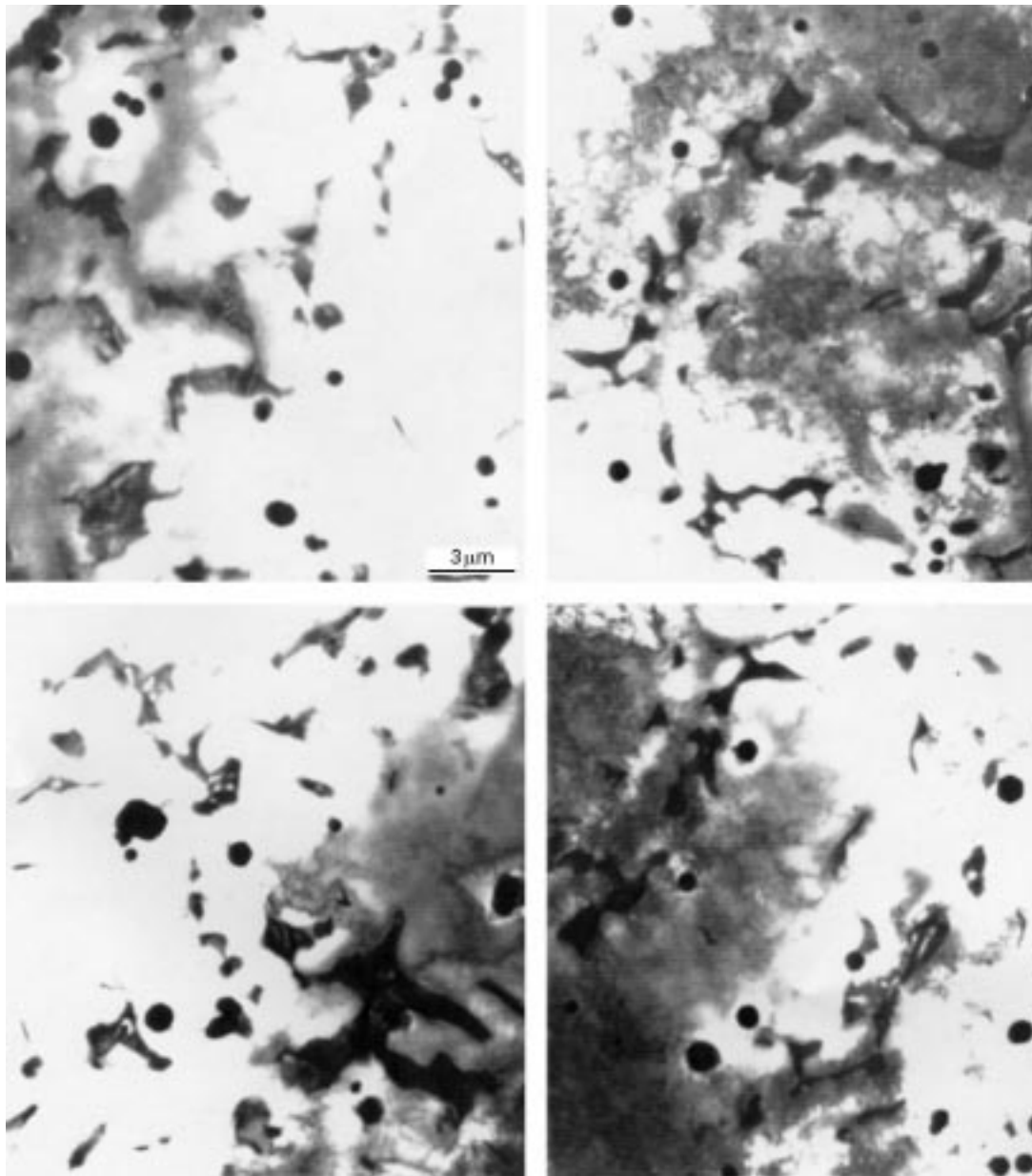


Figure 9 Transmission electron micrograph showing the undissolved hafnium particles in a nickel matrix.

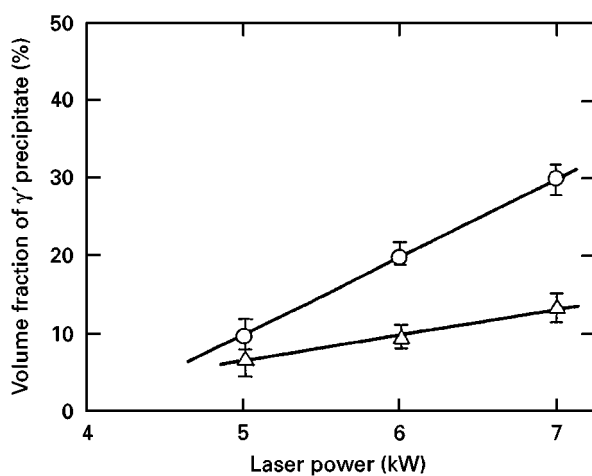


Figure 10 A plot of size variation of fine gamma prime precipitates as a function of laser power at two traverse speeds: (○) 6.35 mm s<sup>-1</sup> and (△) 14.8 mm s<sup>-1</sup>.

Among these ceramic materials, metallic oxide coatings are preferred in the hot section of gas turbine engines because of their high-temperature thermal stability and lower thermal conductivity in the oxygen-enriched environments. Three main types of TBC materials are used in the turbine industries: yttria-stabilized zirconia ( $ZrO_2$ -3 to 8 wt %  $Y_2O_3$ ), alumina-stabilized zirconia ( $ZrO_2$ -3 to 8 wt %  $Al_2O_3$ ) and ceria-stabilized zirconia ( $ZrO_2$ -3 to 8 wt %  $CeO_2$ ). Physical properties of various TBC materials are listed in Table II [20–24]. Yttria-stabilized zirconia is the most common TBC candidate material used in the turbine industry because of its high thermal stability, low thermal conductivity, and high fracture toughness among the oxide ceramic materials [5, 8, 21].

In the ceramic oxide family, maximum durability and thermal stability in thermal barrier coatings were reported in partially stabilized zirconia (i.e.  $ZrO_2$  with 6–8 wt%  $Y_2O_3$ ). In addition, partially stabilized

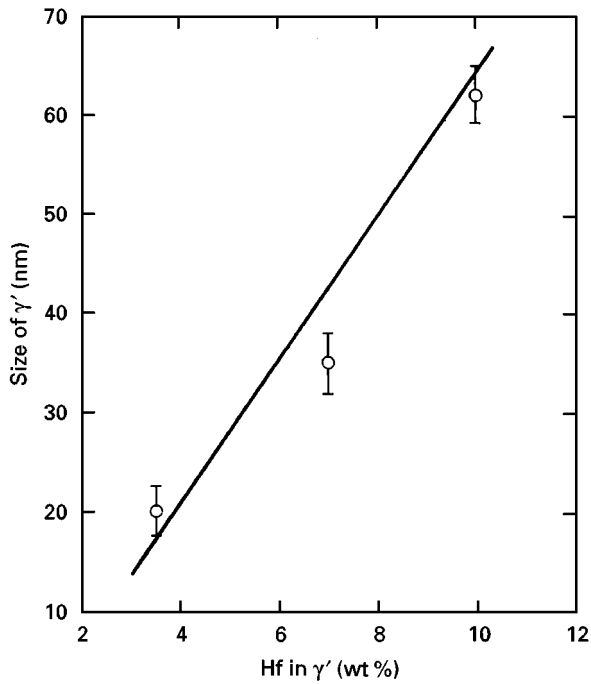


Figure 11 A plot of size variation of fine gamma prime precipitates as a function of hafnium contents.

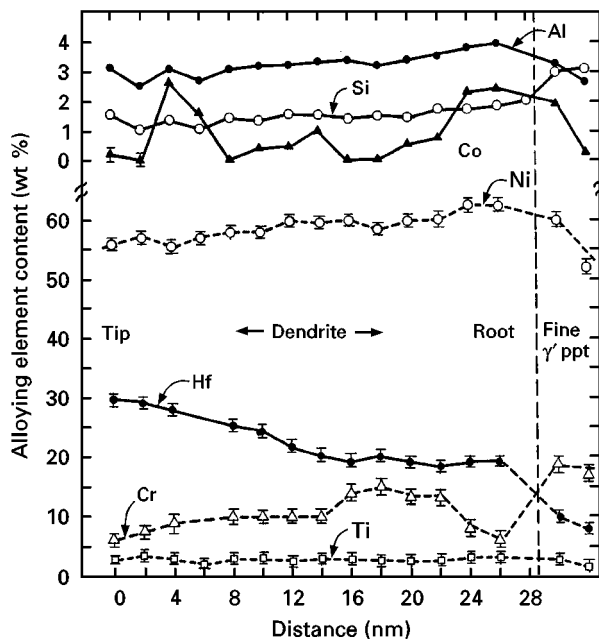


Figure 12 STEM X-ray microanalysis of dendritic growth in the gamma prime precipitates across their growth direction.

zirconia (PSZ) has good fracture toughness, good chemical stability, and the lowest thermal conductivity of any ceramic material [1, 2]. Ceramic coatings are also applied by various techniques including plasma spray, physical vapour deposition (PVD), or chemical vapour deposition (CVD) processes. Before proceeding further, a summary of the physical and mechanical properties of yttria stabilized zirconia and zirconia will be discussed.

Zirconia ( $ZrO_2$ ) has properties such as good mechanical integrity when subjected to thermal shock and

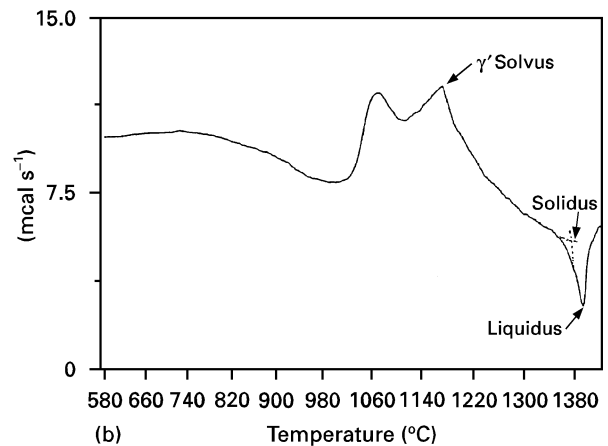
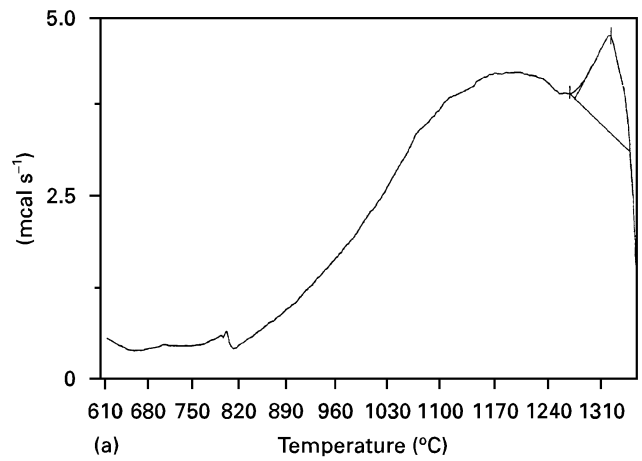


Figure 13 Plots of differential thermal analysis (DTA) of (a) the laser clad alloy and (b) Rene 95 alloy (~1,475 K).

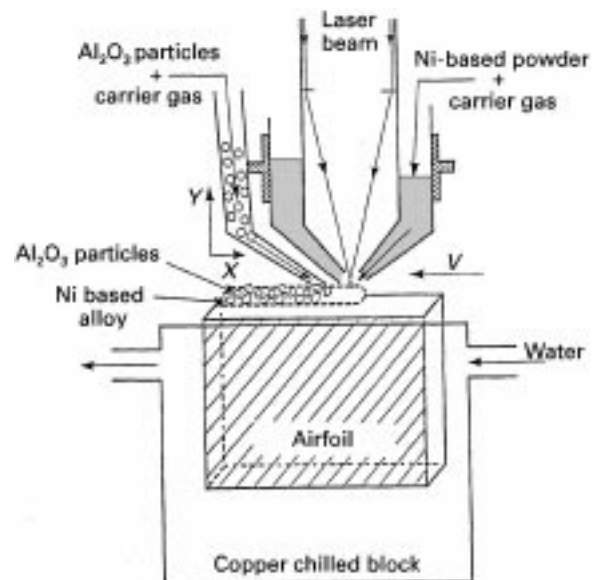


Figure 14 A schematic diagram showing the side delivery of ceramic powder particles into the melt pool region of the substrate.

thermal cycling [9], relatively high thermal expansion coefficient (to match most metals), high thermodynamic stability, high melting temperature, and low thermal conductivity. These characteristics make  $ZrO_2$  the leading material for use as a TBC [10]. However,  $ZrO_2$  undergoes polymorphic phase transformations as the temperature increases. A monoclinic to

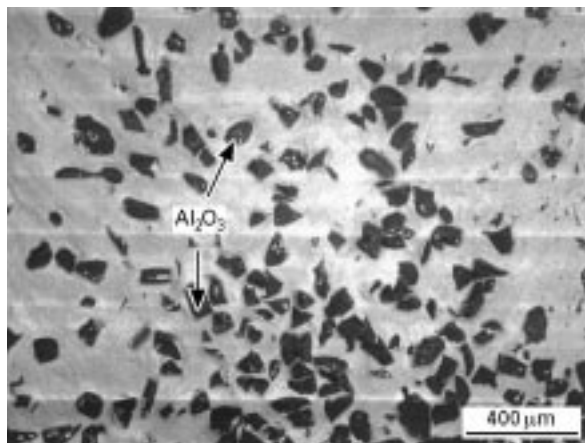


Figure 15 Scanning electron micrograph showing the entrapped ceramic particles in the surface of a laser-clad Ni-Cr-Al-Hf alloy.

tetragonal phase transformation occurs around 1443 K (resulting in a 3–4% decrease in volume) and a tetragonal to cubic transformation around 2643 K [11]. This volume change (during thermal cycling) results in a spalling of the coating, and eventually, component failure. Therefore, to minimize the volume change due to phase transformations at higher temperatures,  $ZrO_2$  is mixed with 3–8 wt% phase-stabilizing agents such as  $CeO_2$ ,  $MgO$ ,  $CaO$ ,  $Al_2O_3$ , and  $Y_2O_3$ .

Among the metallic oxide family, partially stabilized zirconia offers the best physical and mechanical properties that are desired as a coating for high-temperature applications in the turbine industries (Table II). The performance of PSZ as a TBC relies upon the microstructure of the TBC, which depends upon the deposition process, i.e. thermal spray process (plasma spray) or electron beam-physical vapour deposition (EB-PVD).

## 7. TBC evolution – microstructure

The coating industry has undergone vast changes in the last decade and is advancing rapidly. One of the earliest coating processes for thermal barrier coating applications was the plasma spray process. Today, the

leading edge of technology lies with multilayered coatings produced by ion beam-assisted electron beam-physical vapour deposition. In spite of significant advancements in coating technology, industry is continually trying to improve the microstructure, and physical and mechanical properties of TBC (which will have a direct impact in the performance of turbine components). These challenges have sparked a new coating thrust (Fig. 16) as summarized below.

### 7.1. Plasma-sprayed TBCs

The plasma spray process is still commonly used to apply TBC on the hot section of turbine components. Plasma-sprayed TBC often have a porous, lamellar structure containing melted, partially melted and unmelted powder particles [12, 25–27], i.e. a non-uniform microstructure (Fig. 16a). Porosity is needed in TBC applications for accommodating thermal expansion effects during heating and improve thermal shock resistance [28–35]. Owing to the non-uniform microstructure, plasma-sprayed TBC have a low strain tolerance with the metallic substrate, making it difficult to predict the life of coated turbine components. Fig. 17 is a typical micrograph of a plasma-sprayed TBC on a metallic substrate showing a lamellar microstructure with numerous voids. In addition, the bond coat/TBC interface appears to be rough. The bond coat surface is intentionally roughened to improve the degree of adhesion. The adhesion of a plasma-sprayed TBC is primarily governed by the mechanical interlock between the bond coat surface and the TBC. In addition, the roughening of the bond coat surface also induces localized stresses at the bond coat/TBC interface that contribute to the eventual failure of the TBC. Therefore, a balance between adherence and surface roughening (induced stresses) must be made to optimize the life of the TBC. In addition, the surface of the TBC is generally rough. A smooth coating surface is preferred for better air flow in the hot section of the turbine engine.

TABLE II Selected properties of various oxide materials

| Materials | Crystal structure | Coefficient of linear thermal expansion ( $\times 10^{-6} \text{ } ^\circ\text{C}^{-1}$ ) <sup>a</sup> | Melting temperature ( $^\circ\text{C}$ ) | Thermal conductivity ( $\text{cal s}^{-1} \text{ cm}^{-1} \text{ } ^\circ\text{C}^{-1}$ at $100 \text{ } ^\circ\text{C}$ ) |
|-----------|-------------------|--|--|--|
| $ZrO_2$   | Monoclinic        | 9–10   | 2677                                     | 0.0047   |
| $CeO_2$   | Cubic             | 13   | 2600                                     | 0.0260   |
| $Al_2O_3$ | Hexagonal         | 8.8  | 2015                                     | 0.0690   |
| $Y_2O_3$  | Hexagonal         | 9.3  | 2410                                     | –  |
| $MgO$     | Cubic             | 13.5   | 2800                                     | 0.0860   |
| $TiO_2$   | Tetragonal        | 7.1  | 1825                                     | 0.0160   |
| PSZ       | Tetragonal        | 10   | 2730                                     | 0.0043   |
| FSZ       | Cubic             | 7.6–10.6   | 2730                                     | 0.0042–0.0055  |

<sup>a</sup> Above the temperature range 0–1000  $^\circ\text{C}$ , discrepancies exist in the literature for some of these values by as much as 25%. This table reflects the most accepted values for the various materials.

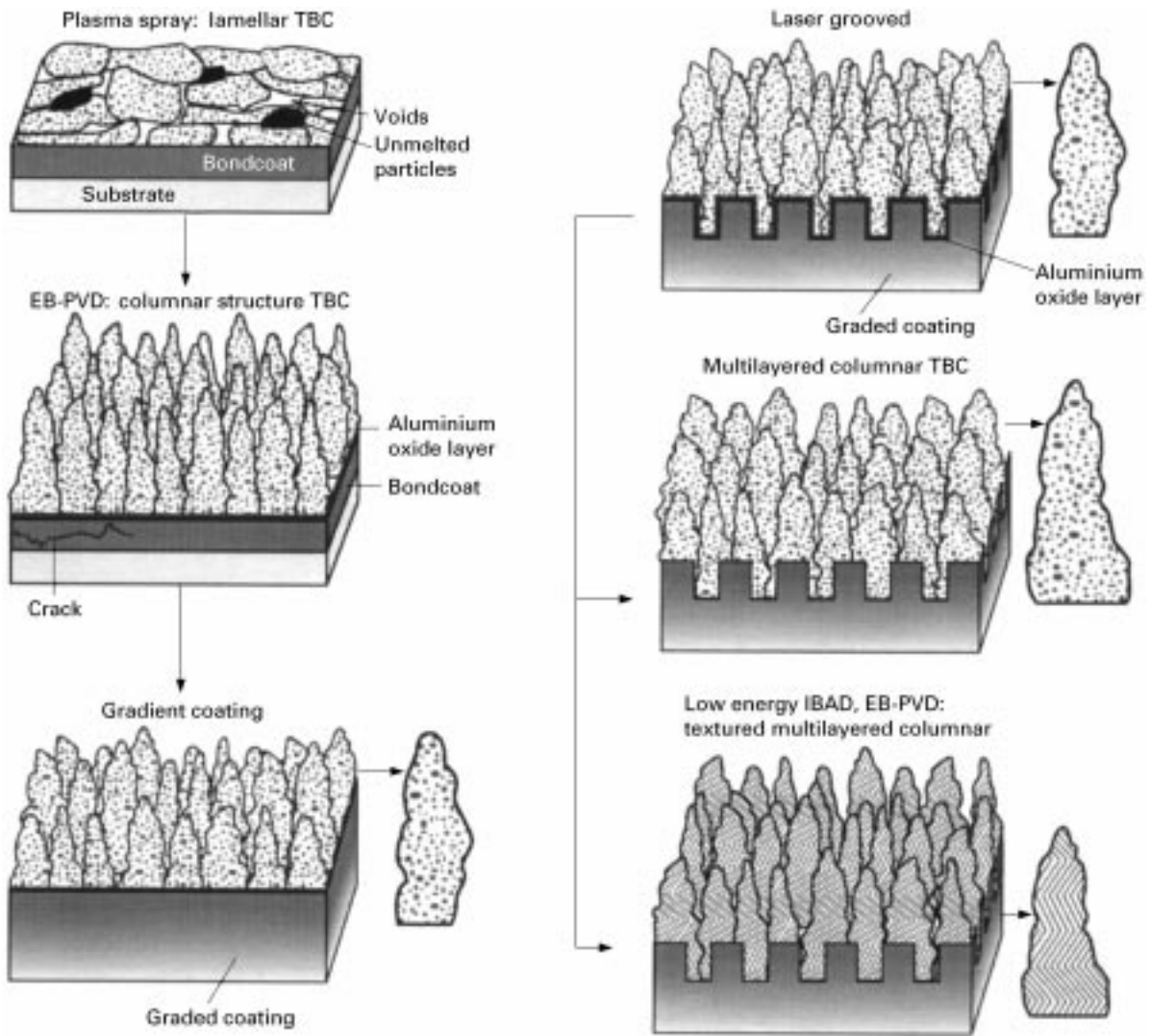


Figure 16 Schematic drawing of the new coating technology thrusts.

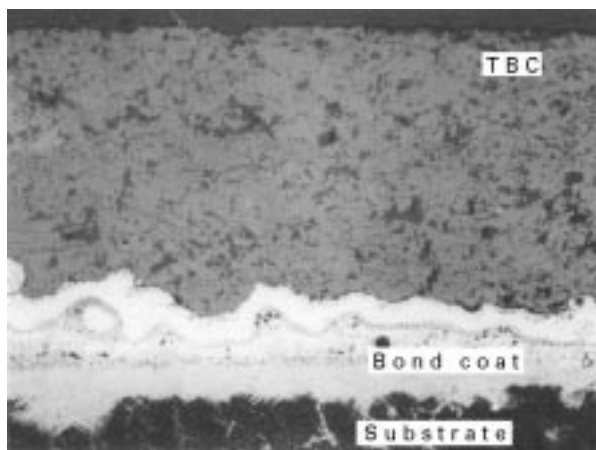


Figure 17 Optical micrograph of a plasma-sprayed, partially stabilized zirconia (PSZ) coating.

## 7.2. EB-PVD TBCs

The turbine industry is interested in an alternative coating process that can offer a uniform and

controlled microstructure in the TBCs [36]. EB-PVD is a cost-effective coating process that can meet the turbine industry requirement. To improve further the performance and reliability of the TBC, the turbine industry prefers to have a columnar microstructure in the TBC rather than a lamellar microstructure (which can only be accomplished by the EB-PVD process). The significant advantage of the columnar microstructure in the TBC is the better strain tolerance between the coating and the substrate (Fig. 16b). Fig. 18 shows the corresponding scanning electron micrographs of the columnar structure of a TBC deposited by the EB-PVD process that has extended the life of turbine components by over 200%. Fig. 18a shows the “mushroom” morphology of the smooth TBC surface common to the EB-PVD process. The smooth surface can be attributed to the diffusion bonding (unlike plasma-sprayed TBC) at the TBC/bond coat interface. At higher magnifications (Fig. 18b–d), a “feather” morphology with striations is observed in the columnar coating. These striations result from non-continuous vapour condensation on the rotating substrate.

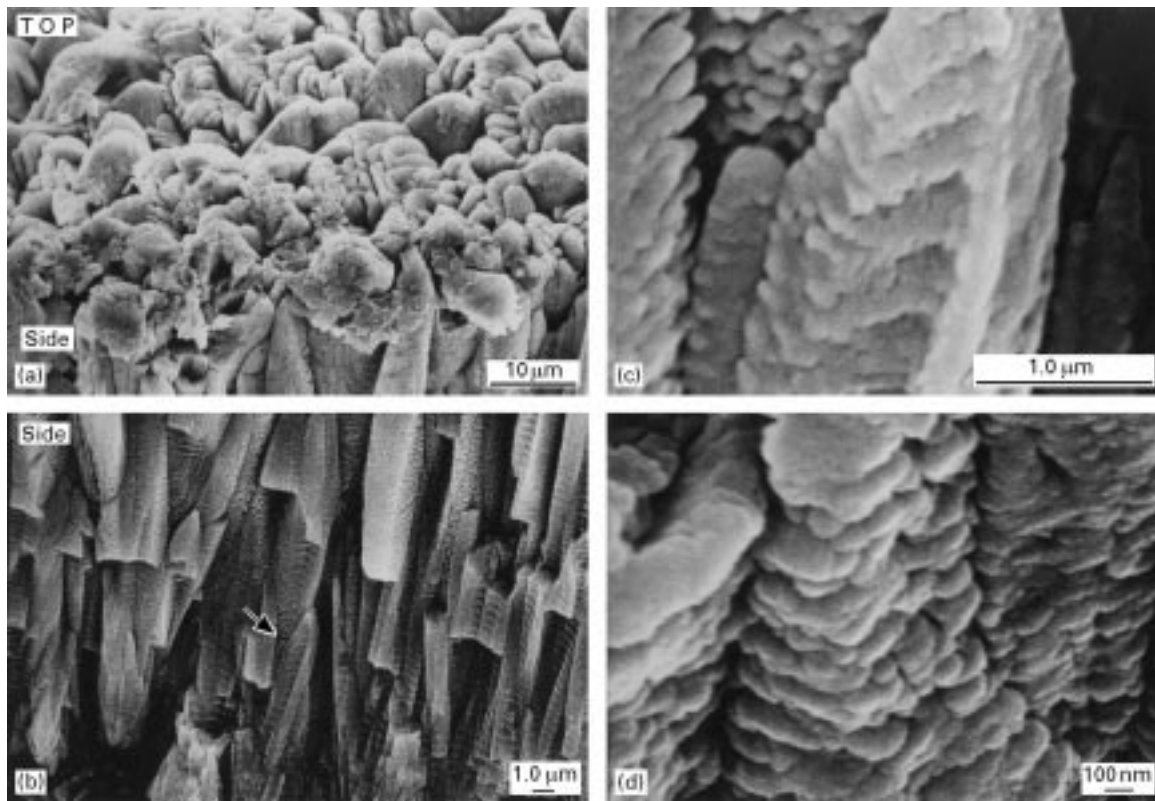


Figure 18 Scanning electron micrographs showing the columnar microstructure of partially stabilized zirconia (PSZ) thermal barrier coating (TBC).

### 7.3. Functional graded coatings

The hot section of turbine components is generally composed of nickel-based alloys. A bond coat, as an intermediate layer, is often applied prior to depositing the TBC to minimize the thermal expansion mismatch between the substrate (nickel-based alloy) and the TBC. The bond coat is generally an MCrAlY alloy (where M = Co, Fe, Ni, or a mixed combination). The bond coat also serves to protect the substrate (metal) from oxidation and corrosion, accommodates stresses induced by differences in thermal expansion, and improves the metallic/ceramic bonding. In spite of using the bond coat as an intermediate layer, coating spallation occurs at the TBC/bond coat interface. Coating spallation is primarily the result of abrupt changes in the microstructure and poor bonding between the TBC and the bond coat.

To improve further the role of the bond coat, the functional graded coating (FGC) concept is being explored in the turbine industry (Fig. 16c). In a FGC, the composition is constantly varied throughout the thickness of the coating. The composition of the FGC can be manipulated in the MCrAlY alloy to reduce the thermal expansion mismatch between the bond coat and the TBC by selectively varying the composition of the constituent elements such as aluminium, nickel and yttrium. In addition, a functional graded bond coat will improve adhesion and produce better thermal and corrosion-resistant properties.

### 7.4. Laser grooving

It has been well documented in the literature that the spallation of the TBC mainly occurs due to the forma-

tion of an oxide layer at the TBC/bond coat interface [37–42]. Owing to residual stresses at the interface, cracks initiate at the TBC/bond coat interface. Debonding of the TBC occurs very rapidly due to the high diffusion of contaminants into the crack region. Thus, a new concept must be developed in order to retard the crack growth mechanism.

The concept of laser engraving the surface of the bond coat (prior to applying the TBC) is being investigated as shown in Fig. 16d. Very limited research has been conducted in this area. However, laser engraving will serve three purposes. First, it will alter the crack growth mechanism that occurs at the TBC/bond interface. Second, the TBC applied on the laser-engraved components will have a better adhesion with the substrate. It is well known that depositing a coating on a smooth surface will often result in delamination when the component is subjected to shear stresses (i.e. rotation). This result means that a smooth surface will have poor bonding. Therefore, roughening the surface of the substrate, or by creating artificial, periodic grooves with a laser on the surface of the substrate will enhance adhesion between the TBC and the substrate (Fig. 16d). However, mechanical roughening over the entire bond coat surface can induce unwanted stresses at the interface. Therefore, laser engraving the bond coat at periodic intervals is preferred. Third, the size of the laser groove (i.e. depth and width) will govern the grain size of the columnar microstructure of the TBC. The grain size of the TBCs plays a significant role in the component's performance that will be discussed in the next section. Fig. 19 shows the columnar microstructure of a yttria-stabilized zirconia coating applied on a laser-engraved

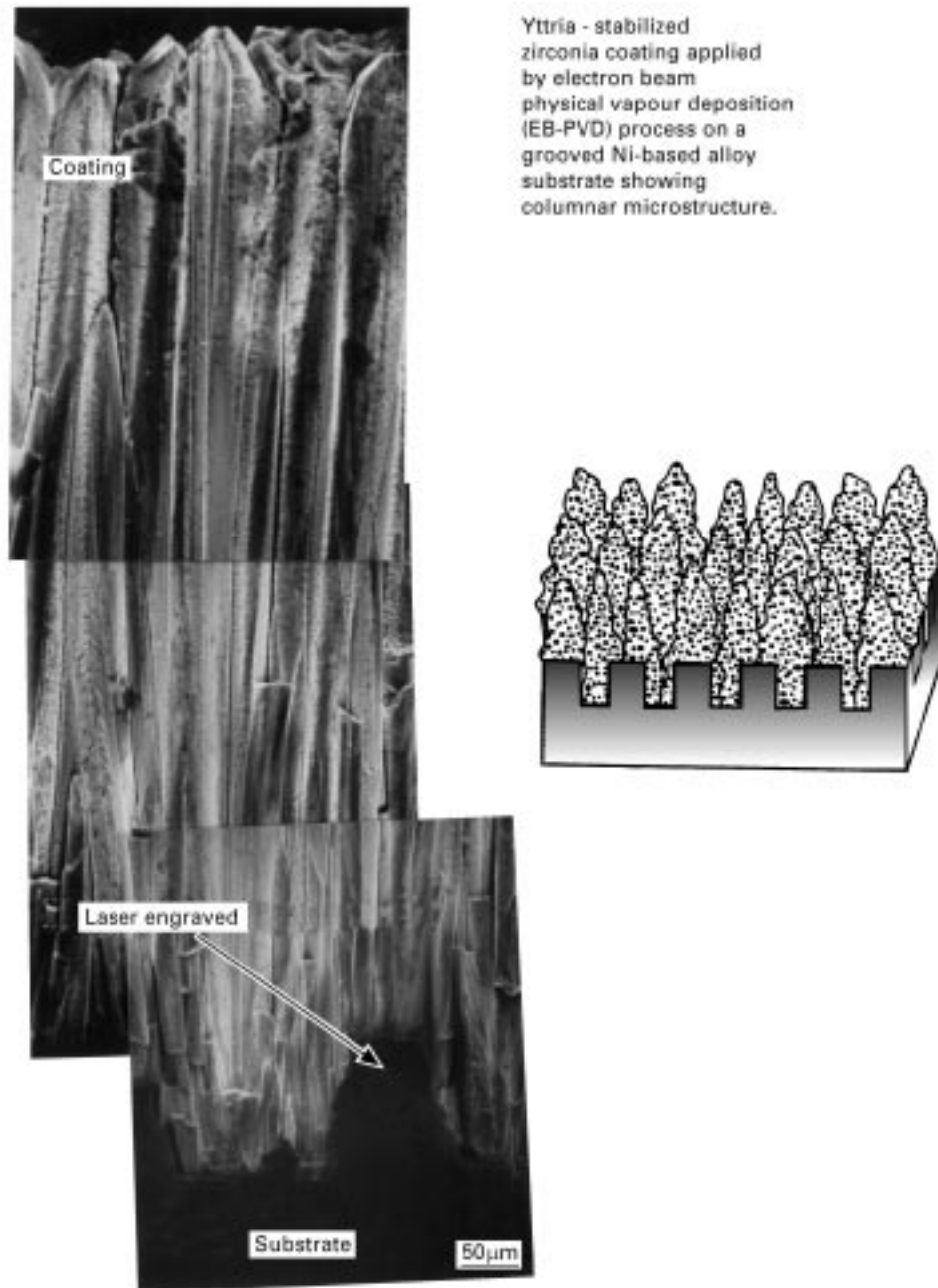


Figure 19 Partially stabilized zirconia thermal barrier coating (TBC) applied by the EB-PVD process on a laser-grooved nickel-based substrate.

nickel-based alloy by the EB-PVD process. The groove is approximately 130 µm deep and 75 µm wide. Combining the formation of a functional gradient bond coat with laser engraving will result in better performance of the TBCs.

### 7.5. Multilayered coatings

Multilayered ceramic and metallic coatings are receiving much attention from researchers in the areas of basic science and advanced technological applications (Fig. 16e). Multilayered coatings will offer unique physical and mechanical properties due to the refined microstructure [43,44]. Multilayered TBC will have advantages from the standpoint of lower thermal conductivity and higher reflectivity than that of the current TBC produced by the conventional

plasma spray or EB-PVD processes. Limited or no research has been conducted in the development of thick, laminated TBC for high-temperature applications. The proper selection of coating material, thickness of layers, and number of layers should provide better thermal resistance as well as wear-resistant properties.

### 7.6. Multilayered textured coatings

The next challenge in the TBC area is to apply cost-effective multilayered textured coatings with a columnar microstructure (Fig. 16e and f). Texturing means growing the film or coating in a preferred orientation. Close-packed planes in a given phase are preferred for controlled mechanical and thermal properties. In addition, the physical and mechanical properties of the

coating depend upon the grain size and grain orientation (i.e. texturing). Thus, texturing would also be beneficial for increasing the wear/thermal resistant properties of TBC.

Texturing in the coating is generally done by incorporating an ion-beam source (i.e. ion beam-assisted deposition, IBAD) into the coating system, and such an example includes the EB-PVD process. The ion-beam source provides additional energy (50–1000 eV) to the vapour cloud (0.1 eV). The resultant energy in the vapour cloud controls the preferred orientation/texture in the coating formation. Textured ceramic coatings have unique physical and mechanical properties. The formation of multilayered textured coatings may not be economical for the turbine industry, but will have specific applications in the high risk and high payoff areas such as NASAs ceramic space shuttle tiles. Texturing coatings such that the direction of the close-packed planes is perpendicular to the wear surface, will increase the wear resistance of the coating in the wear direction and thus life enhancement.

## 8. Conclusion

The life of plasma-sprayed thermal barrier coated (TBC) turbine components is limited by an inhomogeneous microstructure, unmelted particles, voids, and poor bonding with the substrate. To overcome some of these difficulties and meet new challenges, the electron-beam physical vapour deposition (EB-PVD) technology is being exploited. When the same TBC was applied by the EB-PVD process, the life of the component was reported to increase by more than a factor of two due to the columnar microstructure with improved metallurgical bonding with the substrate. The columnar microstructure will ensure better compatibility between the TBC and the turbine components, i.e. the thermal expansion of the turbine components will be in the columnar growth direction of the TBC. The EB-PVD process is highly flexible in producing uniform coatings with a controlled microstructure. In addition, the EB-PVD process is capable of applying various types of ceramic and metallic coatings, including functional gradient coatings, multilayered thick ceramic coatings, and textured multilayered coatings.

Laser cladding is a non-equilibrium process by which the solid solubility limit of the alloying additions can be extended with a refined microstructure. Non-equilibrium alloys have shown a high thermal stability with improved oxidation-resistant properties. Laser cladding is a cost-effective process and can follow the contour of turbine blade tip without any masking.

## References

1. P. VINCENZINI, *Ind. Ceram.* **10** (3) (1990) 113.
2. T. YONUSIIONIS, R. STAFFORD, T. AHMED, L. D. FAVRO, P. K. KUO and R. THOMAS, *Am. Ceram. Soc. Bull.* **71** (1992) 1191.
3. H. HERMAN, *Sci. Am.* **256** (9) (1988) 112.
4. R. W. SMITH and R. KNIGHTS, *J. Metals* **8** (1995) 32.
5. R. MILLER, *J. Eng. Gas Turbines Power* **111** (1989) 301.
6. D. WOLFE and J. SINGH, "Proceedings of 1995 International Electron Beam Conference" edited by R. Bakish, Bakish Materials Corporation, Englewood, New Jersey (1995) pp. 135–146.
7. D. WOLFE, M. B. MOVCHAN and J. SINGH, "Advances in Coatings Technologies for Surface Engineering," edited by C. R. Clayton, J. K. Hirvonen, and A. R. Srivatsa, The Minerals, Metals & Materials Society, Warrendale, Pa (1997) pp. 93–110.
8. S. APPIANO and P. VINCENZINI, *J. Mater. Synth. Process.* **1** (1) (1993) 17.
9. S. STECURA, *Ceram. Bull.* **61** (2) (1982) 256.
10. M. FOUJANET, J. LUMET, J. DEREPA and F. NARDOU, in "Zirconia'88 - Advances in Zirconia Science and Technology", edited by S. Meriani (Elsevier Applied Science, New York, 1988) pp. 89–98.
11. G. INGO, E. PAPAARAZZO, O. BAGNARELLI and N. ZACCHELLI, *Surface Interface Anal.* **16** (1990) 515.
12. R. BUNSHAH, "Handbook of Deposition Technologies for Films and Coatings", Noyes Publications, Park Ridge (1994).
13. J. SINGH, *J. Mater. Sci.* **29** (1994) 5232.
14. *Idem*, *J. Metals* **9** (1992) 8.
15. J. SINGH, B. N. BHAT, R. POORMAN, A. KAR, and J. MAZUMDER, *Surfaces Coat. Technol.* **79** (1996) 35.
16. J. SINGH and J. MAZUMDER, *Acta Metall.* **35** (1987) 1987.
17. J. SINGH, K. NAGANATHAN and J. MAZUMDER, *High Temp. Technol.* **5** (3) (1987) 131.
18. J. SINGH and J. MAZUMDER, *Metall. Trans.* **8** (1988) 1588.
19. C. LYNCH (ed.), "Practical Handbook of Materials Science", (CRC Press, Boston, 1989).
20. W. KINGERY, H. BOWEN and D. UHLMANN, "Introduction to Ceramics," John Wiley & Sons, New York, New York, 1976.
21. S. MEIER, D. K. GUPTA, and K. D. SHEFFLER, *J. Metals*, **43** (3) (1991) 51.
22. D. LIDE (ed.), "Handbook of Chemistry and Physics", 71st Edn, (CRC Press, Boston, 1990).
23. S. SCHNEIDER, J. DAVIS, G. DAVIDSON, S. LAMPMAN, M. WOODS, T. ZORC and R. UHL, "Engineered Materials Handbook-Ceramics and Glasses", Vol. 4 (ASM International), Metals Park, Ohio (1991) pp. 30, 316.
24. J. SHACKELFORE and W. ALEXANDER, "The CRC Materials Science and Engineering Handbook" (CRC Press, Boca Raton) 1994.
25. M. HOCKING, V. VASANTASREE, and P. S. SIDK, "Metallic and Ceramic Coatings", Longman Scientific and Technical, John Wiley & Sons Inc., New York, New York, 1989.
26. P. FAUCHAIS, *Mater. Sci. Monogr.* **67** (1991) 3.
27. P. GILMAN, *J. Metals* **45** (1993) 41.
28. C. BERNDT, *Thin Solid Films* **119** (1984) 173.
29. S. STECURA, "Improved Metallic and Thermal-Barrier Coatings", *NASA Tech Briefs* **5** (1980) 321.
30. N. SHANKAR, H. HERMAN, S. SINGHAL and C. BERNDT, *Thin Solid Films* **119** (1984) 159.
31. P. VINCENZINI, *Ind. Ceram.* **10** (3) (1990) 113.
32. P. HARMSWORTH and R. STEVENS, *J. Mater. Sci.* **27** (1992) 611.
33. *Idem*, *ibid.* **27** (1992) 616.
34. *Idem*, *ibid.* **26** (1991) 3991.
35. L. LELAIT, T. S. ALPERINE, C. DIOT and M. MEVREL, *Mater. Sci. Eng.* **A121** (1989) 475.
36. O. UNAL, T. MITCHELL and A. HEUER, *J. Am. Ceram. Soc.* **77** (1994) 984.
37. B. WU, C. CHAO, E. CHANG and T. CHANG, *Mater. Sci. Eng.* **A124** (1990) 215.
38. B. WU, E. CHANG, S. CHANG and D. TU, *J. Am. Ceram. Soc.* **72** (2) (1989) 212.
39. G. McDONALD and C. HENDRICKS, *Thin Solid Films* **73** (1980) 491.

40. G. KLEER, R. SCHONHOLZ, W. DOLL, S. STURLESE, and N. ZACCHETTI, in "High Performance Ceramic Films and Coatings", edited by P. Vincenzini (Elsevier Science, B.V.), New York, New York (1991) 329–328.
41. E. Y. LEE, R. R. BIEDERMAN and R. D. SISSON, Jr., *ibid.*, (1991) pp. 292–8.
42. D. J. WORTMAN, E. C. DUDERSTADT and W. A. NELSON, *J. Eng. Gas Turbines Power* **112** (1990) 527–530.
43. M. GELL, *J. Metals* **46** (10) (1994) 30.
44. C. AITA, C. SCANLAN and M. GAJDARDZIS-KAJOSIFOVSKA, *ibid.* **46** (1994) 40.

*Received 11 October 1996  
and accepted 2 April 1997*